The high-Q static scattering of 3-methyl pyridine/D_2O mixtures without and with antagonistic salt

Henrich Frielinghaus[1,*], *Purushottam S.* Dubey[1], *Eunjoo* Shin[3], *Mary* Odom[4], *Piotr* Zolnierczuk[4], *Baho* Wu[1], *Olaf* Holderer[1], *Theresia* Heiden-Hecht[1], *Jan V.* Sengers[5], and *Stephan* Förster[1]

[1]Forschungszentrum Jülich GmbH, Jülich Center for Neutron Scattering JCNS-4 at MLZ, Lichtenbergstrasse 1, 85747 Garching, Germany
[2]Korea Atomic Energy Research Institute, 111, Daedeok-daero 989beon-gil, Yuseong-gu, Daejeon, 34057, Republic of Korea
[3]Neutron Sciences Directorate, Oak Ridge National Laboratory (ORNL), POB 2008, 1 Bethel Valley Road, Oak Ridge, TN 37831, USA
[4]Institute for Physical Science and Technology, University of Maryland, College Park, Maryland 20742, USA

Abstract. Here we focus on the high-Q small-angle neutron scattering where we observed deviations from an ideal power law Q^{-2}. From theory, this deviation Δ arises from the critical correlation-function exponent η_d in d dimensions. The investigated systems were 3-methyl pyridine/D_2O without and with antagonistitc salt. They display the critical behavior of a 3d and 2d Ising system, respectively. In the first case, the value of Δ matches the ideal value η_3 well, but in the latter case the value of Δ is affected by the two confined dimensions *and* the third dimension.

1 Introduction

We have studied the critical dynamics of the system 3-methyl pyridine (3MP) / D_2O without and with antagonistic salt [1]. We found a 3d- and 2d-Ising behavior in the static structural measurements (also firstly found in [2, 3]) and a characteristic critical behavior for the dynamics [1]. At large length scales the hydrodynamic diffusion and at small length scales the critical diffusion was observed. While at large length scales whole domains are diffusing, at small length scales an exchange between domains occurs. The two behaviors have a footprint of a dynamic critical exponent $z = 0.063$ and virtually 0, respectively. More important is the difference in the measured bare viscosities between the 3d and 2d cases that also affects the amplitudes for critical dynamics. The 2d confined liquid displays the well-known lubrication effect that goes in hand with the lower bare viscosities.

The understanding of the confinement is based mainly on the theory of Onuki [4–6]. A sketch of the situation is displayed in Fig. 1. The charges mainly form layers and the different ions are found in the domains of 3MP and D_2O. They also serve as wavefronts for the charge density waves and are responsible for the 2d confinement of 3MP/D_2O. The solvation effect described by Onuki means that a rather sharp boundary between 3MP and D_2O domains at this interface leads to strong enrichments, whereas in the other directions the transitions between domains are rather soft. On the other hand, the system without salt is assumed to be a rather ideal 3d Ising system.

*e-mail: h.frielinghaus@fz-juelich.de

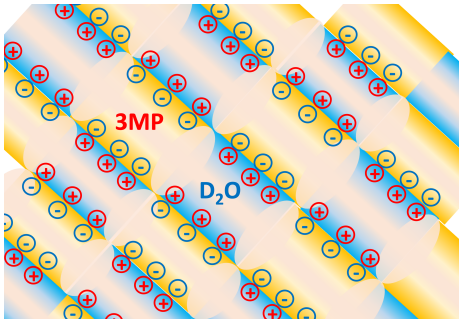

Figure 1. A sketch of the arrangement of the domains of 3MP and D_2O and the ions of the antagonistic salt. The charges are aligned in planes throughout the sample and serve as wavefronts of the charge density waves. The solvation effect is exaggerated by the blue and orange colors (water and 3MP) in terms of a fast decay towards mixing indicated by the light brown color.

By evaluating the high-Q small-angle scattering we look at the phase boundaries just with an orientational average. We first evaluate the asymptotic power laws of the small-angle scattering and then discuss the obtained exponents. Then we summarize and discuss the findings in the context of existing theories.

2 Theory

The classical theory for critical fluctuations in three dimensions is the Ornstein-Zernike theory [7–9], which yields a very simple formula for the scattering, i.e., the

Table 1. Summary of the critical exponent η_d in d dimensions.

dimensionality d	3	2	1
η_d	0.033	$\frac{1}{4}$	$\frac{1}{2}$
citation	[10]	[11]	[12]

correlation function in reciprocal space:

$$S(Q) = \frac{S(Q=0)}{1+\xi^2 Q^2} \tag{1}$$

The real space correlation function then is obtained by a Fourier transform after:

$$G(r) = \frac{1}{4\pi\rho R^2}\frac{\exp(-r/\xi)}{r} \tag{2}$$

Here ρ is the density, and R^2 is the second moment of the direct correlation function $C(r)$ [7]. This approach is widely used and works well for small Q when only the correlation length is extracted from scattering experiments. However, at large Q, there could be deviations from this ideal behavior as Fisher pointed out [7]. He generalized the real space correlation function by including a correction with the critical exponent η_d. The real-space correlation function then reads:

$$G(r) \sim \frac{\exp(-r/\xi)}{r^{d-2+\eta_d}} \tag{3}$$

The general case for d dimensions is covered here. Of course also η_d depends on the number of dimensions. A list of values for η_d can be found in Table 1. We tabulate the classical values that have been established for 3 to 1 dimensions [10–12]. They compare quite well with the values obtained from a Renormalization-Group expansion that depends on $\epsilon = (4-d)$ according to $\eta_d = 0.050\epsilon^2$ [13]. Fisher then proposed a simple corrected formula for the scattering function in three dimensions that reads [7]:

$$S(Q) = \frac{S(Q=0)}{(1+\xi^2 Q^2)^{1-\eta_3/2}} \tag{4}$$

Similarly, one could write a scattering function for two dimensions (that is exact for $\eta_2 = 0$):

$$S(Q) = \frac{S(Q=0)}{\left(\sqrt{1+\xi^2 Q^2}\right)^{1-\eta_2}} \tag{5}$$

One has to be cautious with eqs. 4 and 5 because they give the impression to be exact over the entire Q-range. At small Q, the corrections of η_d are small in the sense that they are nearly invisible (an analytic analysis is presented in the Appendix). At large Q, the asymptotic scaling is correct and then reflects the low-r dependency of eq. 3. However, the prefactor might change and is then different from the low-Q behavior. The medium Q-range is actually not very well known, and usually needs more delicate discussion. This overall mismatch is more pronounced the bigger the exponent η_d is.

For completeness, we summarize the scattering law that was applied to the 3MP/D_2O system with antagonistic salt. The ions were taken into account and one arrives at [2]:

$$S(Q) = \frac{S(Q=0)}{1+\left\{1-\kappa^2/\left(1+\lambda_D^2 Q^2\right)\right\}\cdot\xi^2 Q^2} \tag{6}$$

This function was derived from the real-space correlation function of Onuki [4, 5]. It employs the Debye length $\lambda_D = 39.25$Å as a fixed parameter, and the parameter κ. When $\kappa < 1$ the system is more like a two-component system, and $\kappa > 1$ includes the amphiphilicity of the antagonistic salt with a preferred wavelength of the charge density waves (see [2]). For the current manuscript, we are only interested in the asymptotic Q^{-2} scattering that starts at $Q > 10^{-3}$Å^{-1} where the correlation length ξ is determined and further on might show deviations from the ideal Q^{-2} behavior.

3 SANS data evaluation at high Q

The experiments have been described in the main paper [1]. We just mention that the small-angle neutron scattering (SANS) data have been collected at the Hanaro reactor in the Republic of Korea. Examples for the 3MP/D_2O mixtures are displayed in Fig. 2. While at small Q we can extract the critical behavior, we now focus on the large-Q scattering. We applied the following behavior for the macroscopic cross section (i.e., the calibrated intensity) as a function of the scattering vector Q:

$$\frac{d\Sigma}{d\Omega}(Q) = \frac{A}{Q^{2-\Delta}} + b_{\text{background}} \tag{7}$$

The amplitude A was kept as a free parameter and was not connected to the forward scattering. The exponent Δ describes the difference from the ideal scattering law; and $b_{\text{background}}$ describes the incoherent background (also a free parameter). In the following we focus on the exponent Δ

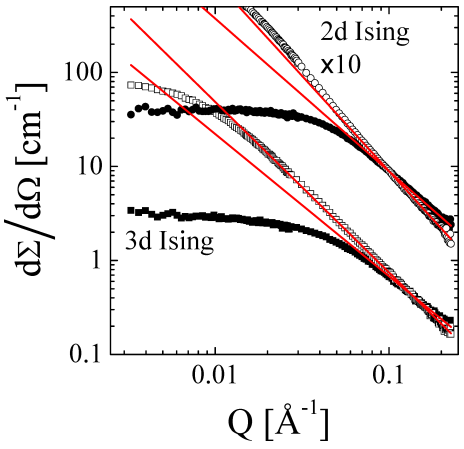

Figure 2. The macroscopic cross section (with background subtracted) as a function of the scattering angle Q for the system 3MP/D_2O (3d Ising system) and 3MP/D_2O with antagonistic salt (2d Ising system, multiplied by 10). The solid symbols indicate a temperature of 20°C and the open symbols the highest temperature of 36°C and 40°C, respectively. The asymptotic high-Q scattering is fitted at $Q > 0.104$Å^{-1} (red lines).

only as the deviation from the ideal behavior. We applied this in the 3d and 2d Ising case in the same manner independent on the dimensionality. The parameter Δ is shown as a function of temperature in Fig. 3. We can see that the temperature dependence is quite linear for temperatures below 32°C (or 34°C). These values are also considerably higher than what would be expected for 3 dimensions, i.e., η_3. The reason for the decay towards higher temperatures is the importance of the incoherent background. We cannot exactly motivate a reason for a linear behavior and so we consider this as an experimental observation. At even higher temperatures there are four data points that are considerably higher than the linear approach. Here, we consider the values to originate from the intermediate Q-scattering where extrapolations become difficult. From the linear extrapolations to $T = T_C$, the critical temperature of 36.9°C (42.9°C), we obtain the exponent $\Delta = 0.043 \pm 0.04$ (-0.292 ± 0.026) at the critical temperature where background issues should be minimal. For the 3d Ising system our result is consistent with the expectation for the critical exponent η_3, except that the statistical errors are nearly larger than the value itself. The negative Δ of the 2d system indicates an incorrect estimate of the ideal asymptote. So we would like to propose the following formula for high Q:

$$S(Q) \sim \frac{1}{\left(\sqrt{1+\xi^2 Q^2}\right)^{1-\eta_2}} \cdot \left|\frac{\sin(QD)}{QD}\right|^{2-\eta_1} \qquad (8)$$

This reflects the critical behavior in the 2 dimensions between the charge density wave fronts (first term), and the sharply defined domains in the third dimension. We also assume a criticality in the direction of the third dimension using η_1. The factorization of two formfactors (critical fluctuations in two dimensions, i.e. eq. 5, and a compact object in the third dimension) does either hold for a separation of length scales [14] or for large polydispersities as in our case. Due to the polydispersity of the domian sizes D in the third dimension, we can replace the oscillatory part $\sin^2(QD)$ by $\frac{1}{2}$ [15]. So, we would correct the original Δ into:

$$\Delta_{\mathrm{corr}} = 3 - 2 + \Delta = 0.708 \pm 0.026 \approx \eta_2 + \eta_1 = \frac{3}{4} \qquad (9)$$

For the values of η_d we refer to Table 1. So, we can state that in the high-Q behavior a strong influence of the one dimension along the propagation of the charge density waves is visible. The contribution of η_1 is stronger than from the other two dimensions in the lateral directions. This is surprising because the criticality of the structural static measurements (at low Q) and the critical dynamics do not display any influence of this separated third dimension. We argued [1] that the finite viscosity that applies for the two lateral dimensions manages to avoid the third dimension for shorter times (when one could speculate about the Pomeau divergence [16]) but at later stages the molecules enter the third dimension when the charge density waves come into play. In the experiments with strong contrast between 3MP and D_2O the whole influence of the charge density waves appears rather low. So it is even more interesting that the third dimension also comes into play at the high-Q static scattering.

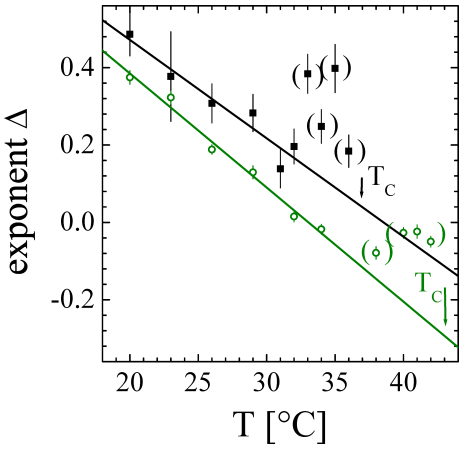

Figure 3. The deviation of the exponent from the ideal value 2 arising from the high-Q SANS power law scattering. This deviation Δ is plotted as a function of temperature. From smaller temperatures towards higher temperatures the trend seems to be linear and then suddenly breaks off to higher values (in brackets). The limit of the linear trend at the critical temperature T_C is determined to be compared to the theoretical exponents η_d.

The one-dimensional Ising criticality is a quite interesting subject. For instance many critical exponents seem to diverge when approaching the dimensionality one [17] (and references herein). For instance the critical exponent ν goes with $\nu = \epsilon^{-1} - \frac{1}{2} + \frac{1}{2}\epsilon + O(\epsilon^2)$ with ϵ being the difference to the ideal one-dimensional case [18]. Thus it is surprising that the exponent η_1 stays finite. A more detailed study of our system would possibly give new insight about other critical exponents in one dimension.

4 Summary

We analyzed the high-Q SANS patterns of 3MP/D_2O mixtures without and with antagonistic salt. Here, we determined the effective exponent from the scattering data that deviates from the ideal exponent of 2. The deviation of this exponent to the ideal case of 2 was then plotted as a function of temperature. We observed a linear behavior at lower temperatures while at elevated temperatures the medium Q-range behavior does not match anymore. The exponent was then extrapolated towards the critical temperature T_C. These values were then compared to the theoretical values of the exponent η_d. For the 3d Ising case the extrapolation matches the ideal 3d-case. For the 2d Ising case we had to derive the ideal power law with an exponent 3, and the deviation Δ_{corr} is affected by the two dimensions where the domains are confined to and the last, third dimension, in which the charge density waves propagate. The last influence is surprising because the charge density waves seem to be not that dominating in the SANS patterns.

In the future the alignment of the charge density waves would be desireable – be it in a shear field or in an electric or magnetic field. Then, the decomposition of different

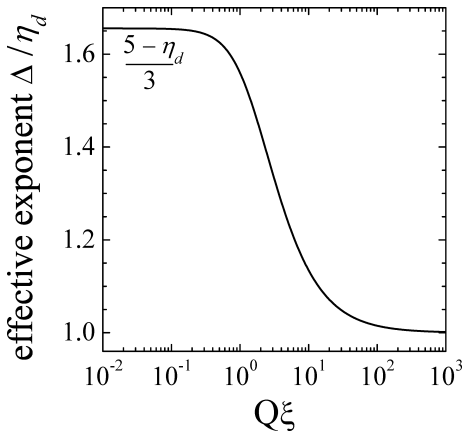

Figure 4. The effective exponent Δ as a function of the parameter $Q\xi$ normalized to the actual exponent η_d (here we assumed the 3-dimensional case, that is the only known analytic and exact solution given in eq. 10). However, for other dimensionalities we expect an extremely similar behavior.

terms would be easier and the exponent η_1 would appear isolated.

5 Appendix

From eq. 3 we could derive the scattering function in three dimensions exactly:

$$S(Q) \sim \frac{\cos(\eta_3 \arctan(Q\xi)) - \sin(\eta_3 \arctan(Q\xi))/(Q\xi)}{(1+Q^2\xi^2)^{1-\eta_3/2}} \tag{10}$$

The enumerator contains the details about the transition from small $Q\xi < 1$ to large $Q\xi > 1$. The amplitudes and effective exponents (or slopes) change between the two cases. The effective exponent Δ at a specific $Q\xi$ normalized to the actual exponent η_d is displayed in Fig. 4. It decays from a maximum at small $Q\xi$ towards the expected ratio unity at large $Q\xi$. This also means that the intensities (or the effective amplitude) at small $Q\xi$ are smaller and a faster decay towards higher $Q\xi$ is observed (most curves in Fig. 2 stay below the high-Q power law, and only for the 2d-Ising case at 40°C the deviation is reversed - possibly due to the charge density waves, see eq. 6). Thus we believe that the enumerator of eq. 10 might be seen as a general switching function between the two Q-regions also for other dimensionalities. However, for different dimensions the exact expressions are not analytic anymore.

References

[1] H. Frielinghaus, P.S. Dubey, B. Wu, M. Odom, F. Zheng, E. Shin, P. Zolnierczuk, O. Holderer, S. Förster, T. Heiden-Hecht, Phys. Rev. Res. **5**, 023053 (2023)

[2] K. Sadakane, N. Iguchi, M. Nagao, H. Endo, Y.B. Melnichenko, H. Seto, Soft Matter **7**, 1334 (2011)

[3] K. Sadakane, M. Nagao, H. Endo, H. Seto, The Journal of Chemical Physics **139**, 234905 (2013)

[4] A. Onuki, H. Kitamura, The Journal of Chemical Physics **121**, 3143 (2004)

[5] A. Onuki, The Journal of Chemical Physics **128**, 224704 (2008)

[6] D. Jung, N. Rivas, J. Harting, The Journal of Chemical Physics **150**, 064912 (2019)

[7] M.E. Fisher, Journal of Mathematical Physics **5**, 944 (1964)

[8] F. Leclercq, S. Pouget, P. Damay, in *Neutron Spin Echo Spectroscopy: Basics, Trends and Applications* (Springer, 2002), pp. 232–245

[9] H. Frielinghaus, D. Schwahn, J. Dudowicz, K.F. Freed, K. Foreman, The Journal of Chemical Physics **114**, 5016 (2001)

[10] M. Anisimov, J. Sengers, Supercritical Fluids: Fundamentals and Applications pp. 89–121 (2000)

[11] A. Pelissetto, E. Vicari, Physics Reports **368**, 549 (2002)

[12] Y.W. Dai, X.H. Chen, S.Y. Cho, H.Q. Zhou, D.X. Yao, arXiv preprint arXiv:1805.03464 (2018)

[13] G.R. Golner, Physical Review B **8**, 339 (1973)

[14] J.S. Pedersen, P. Schurtenberger, Macromolecules **29**, 7602 (1996)

[15] M. Wagener, S. Förster, Scientific Reports **13**, 780 (2023)

[16] Y. Pomeau, Physical Review A **5**, 2569 (1972)

[17] M. Novotny, Physical Review B **46**, 2939 (1992)

[18] D. Forster, A. Gabriunas, Physical Review A **23**, 2627 (1981)